

# A Cost-Efficient LED Driver with Low-Flicker

Chih-Lung Yang<sup>1</sup>, Y.T. Yau<sup>2\*</sup>

## ABSTRACT

The market for LED lighting has been growing steadily due to its high efficiency and long life. However, there are still several technical challenges to overcome, especially with grid-powered LED drivers. The line-frequency flicker has become a health issue. Although line-frequency flicker is usually invisible, it can be picked up by the retina, causing visual fatigue. Therefore, LED drivers need to produce constant power to avoid flicker. In this paper, a hybrid driver circuit with an isolated PFC flyback and a linear constant current LED driver is proposed with the novel dynamic control method. The new approach enables the linear constant-current LED driver to operate with high efficiency. Since the linear constant-current LED driver has no concern about high-frequency, high-voltage, and high-current switching. It minimizes EMI risk and reduces the system complex and cost. Finally, a low flicker 25W LED driver with DALI 2.0 interface is completed.

**Keywords:** LED, flicker, lighting

## 1. INTRODUCTION

The market for LED lighting has been growing steadily due to its high efficiency and long life. However, there are still several technical challenges to overcome, especially with grid-powered LED drivers. The line-frequency flicker has become a health issue. Although line-frequency flicker is usually invisible, it can be picked up by the retina, causing visual fatigue (Wilkins, Veitch & Lehman, 2010). Therefore, LED drivers need to generate constant power to avoid flicker. Therefore, LED drivers need to produce constant power to avoid flicker (Liu et al., 2015). Various LED driving methods have been investigated to achieve flicker-free performance. Some studies have focused on control strategies (Gao, Li & Mok, 2015; Wang et al., 2011; Li, Han & Sanders, 2018; Fu et al., 2018), while common two-stage LED drivers can achieve flicker-free LED driving. There are also many studies that focus on power supply topologies (Cheng, Cheng & Chung, 2014; Dong et al., 2014; Fang & Liu, 2014, 2016; Fang et al., 2013; Fang et al., 2016; Fang et al., 2018; He, Ruan & Zhang, 2016; Hu & Zane, 2010; Hu & Zane, 2011; Wang, Zhang & Qiu, 2017; Yang et al., 2013; Yan et al., 2014;). For example, the harmonic current injection method reduces the unbalanced energy during half a line-frequency (Ruan et al., 2010). The second DC-DC converter in a conventional PFC-DC/DC two-stage topology can effectively filter out line-frequency flicker, but the disadvantages of the two-stage design are increased losses in the additional power stage, more EMI risk, and higher cost.

This paper proposes a hybrid driver circuit with an isolated PFC flyback and a linear constant-current LED driver. The novel approach enables the linear constant-current LED driver to operate with high efficiency. Since the linear constant-current LED driv-

er operates without high-frequency, high-voltage, high-current switching, and any magnetic component, it minimizes EMI emissions and reduces the system complex and costs. The final result is a 25W LED driver with low-frequency flicker.

## 2. SYSTEM STRUCTURE

Fig. 1 shows the two-stage topology. The PFC flyback provides power factor correction and satisfies electrical isolation requirements. It also generates significant line-frequency voltage ripple on the output capacitor  $C_{O1}$ . Two magnetic components,  $T_1$  and  $L_O$ , two power rectifier diodes,  $D_{O1}$  and  $D_{O2}$ , two power switches  $Q_1$  and  $Q_2$ , and two converter control ICs,  $U_1$  and  $U_3$  are required.

Fig. 2 shows the PWM dimming method and the analog dimming method. The PWM dimming method of the two-stage structure has the advantages of simple design, wide dimming range, and easy digital interface. The LED driving current is between 0% and 100%, and the large current amplitude is the main cause of high-frequency flicker. However, the significant advantage of analog dimming is flicker-free.

Fig. 3 shows the new driving concept proposed in this paper, replacing the switching DC-DC converter in Fig. 1 with a linear constant current source  $i_{source}$ . The output of the feedback compensator,  $v_E$ , drives the low-power NPN transistor  $Q_3$ , which instantly adjusts the flyback compensation voltage divider networks  $v_F$  and  $v_G$ , and then instantly controls the output voltage  $v_A$  of the flyback converter.

The  $i_{source}$  is based on the characteristics of MOSFETs [1], as shown in Fig. 4, the MOSFETs are operated in the saturation region, and proper control of MOSFETs above  $v_{ds} > v_{ds-min}$  will ensure that the  $i_{source}$  is not affected by variation on  $v_{ds}$ . As shown in Fig. 5, for further design details of the constant current source, the relevant circuit can be found in [2], using the operational amplifier  $OPA_2$  for negative feedback control of the  $v_C$  signal,  $i_{LEDs} = (i_{ref}/R_S)$ . This constitutes the feedback compensator of  $i_{source}$ . Assuming a constant value of  $V_{LEDs}$  across the LED string, the  $v_B$  and  $v_{ds}$  are shown in (1) and (2).  $v_{A-max}$  is  $v_A$  at the high point of the ripple.

Manuscript received June 10, 2022; revised June 26, 2022; accepted July 5, 2022.

<sup>1</sup> Senior Engineer, Asian Power Devices Inc., Taoyuan, Taiwan.

<sup>2\*</sup> Assistant Professor (corresponding author), Department of Electrical Engineering, National Chin-Yi University of Technology, Taichung, Taiwan. (pabloyau@ncut.edu.tw)

$$v_B = v_A - V_{LEDs} \quad (1)$$

$$v_{ds} = v_B - v_C = v_B - i_{LEDs} \cdot R_S = v_A - V_{LEDs} - i_{LEDs} \cdot R_S \quad (2)$$

According to the [2],  $i_{source}$  can be designed to maintain  $v_{B-min} \geq V_{ref}$ . The target is to dynamically keep  $v_{B-min} = V_{ref}$  to achieve the minimum loss.  $v_{ds-min}$  can therefore be calculated as in (3).

$$v_{ds-min} = v_{B-min} - i_{LEDs} \cdot R_S \quad (3)$$

According to datasheet [3] of  $Q_2$ ,  $V_{ref}$  is designed to be 0.6 V with  $i_{LEDs} = 0.45$  A,  $R_S = 0.39 \Omega$ , and  $v_{ds-min} = 0.42$  V.

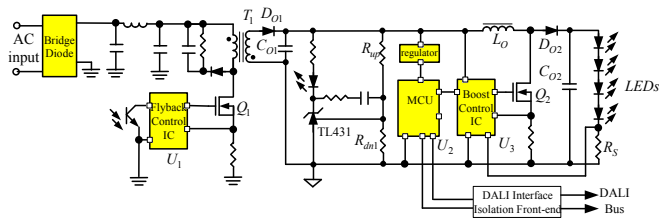


Fig. 1 Typical traditional two-stage LED driver structure with low-frequency flicker

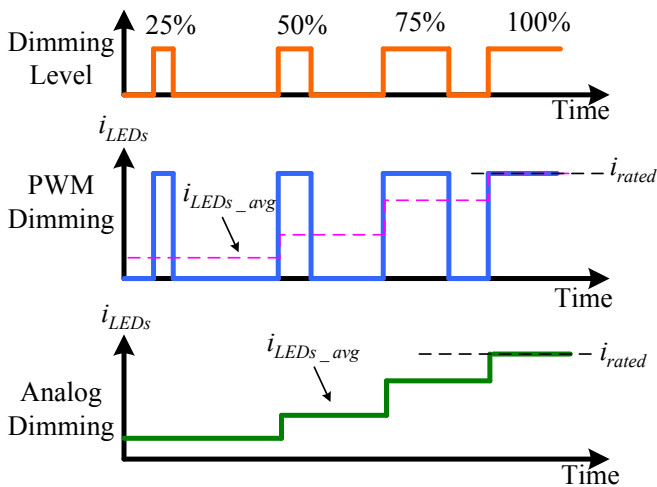


Fig. 2 PWM and analog dimming methods

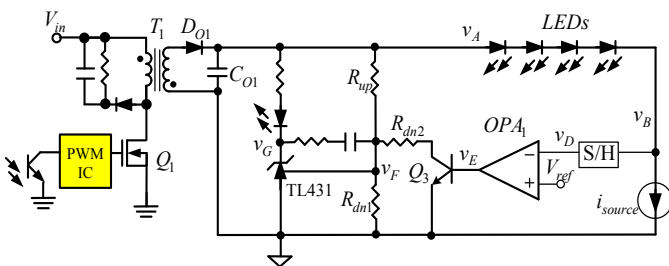


Fig. 3 The proposed concept with low flicker

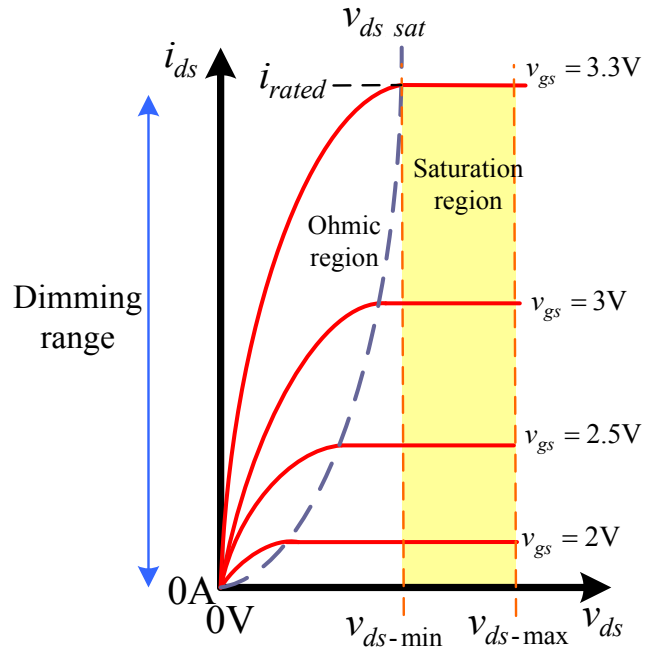


Fig. 4 Typical output characteristics of N-channel power MOSFET<sup>[2]</sup>

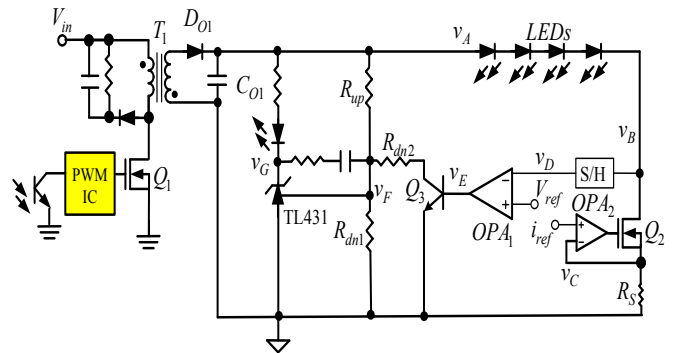
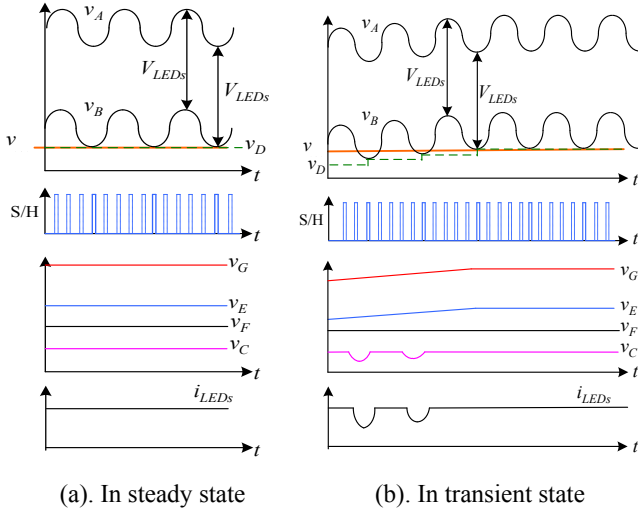


Fig. 5 The proposed LED driver circuit

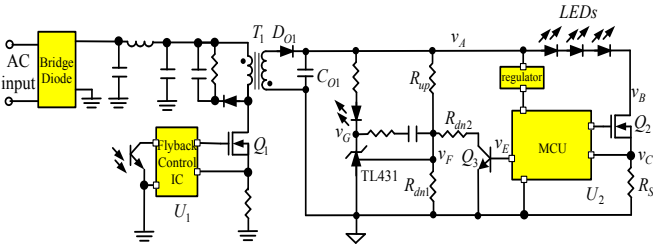
Fig. 6(a) shows that when the circuit is operating at a steady state, the sample and hold (S/H) function samples  $v_B$  with at least 20 times the line frequency to detect the valley position.  $v_{B-min}$  is selected as  $v_D$ , and  $v_D$  is used to amplify and compensate for the feedback error with  $V_{ref}$  to control  $v_E$ ,  $v_F$ , and  $v_G$  to control  $U_1$  and change  $v_A$ .

Fig. 6(b) explains the dynamic behavior at each point. When  $v_{B-min}$  is under  $V_{ref}$ ,  $i_{source}$  is unstable and generates flicker. The result of  $v_D < V_{ref}$  makes  $v_E$  rise so that  $R_{dh2}$  current increases, which makes  $v_F$  fall and  $v_G$  rise, then  $U_1$  increases the duty cycle of  $Q_1$  so that  $v_A$  increases. Finally,  $v_A$  will rise to make  $v_{B-min} = v_D = V_{ref}$ . Then,  $v_{B-min}$  returns to a steady state to maintain  $i_{source}$  to a stable operation.



**Fig. 6** Waveforms of the proposed low-frequency flicker drive structure at each point

Fig. 7 shows the actual circuit implementation.  $OPA_2$  is an internal block of the MCU. The sample and hold function and  $OPA_1$  is realized by internal ADC and software code.  $Q_3$  is a small-signal NPN BJT transistor. Therefore, the actual constant current source  $i_{source}$  needs a few number of components.  $Q_2$ ,  $R_S$ , and  $Q_3$  are new additional components for building the constant current source  $i_{source}$ .



**Fig. 7** The actual structure of the proposed LED driver

Table 1 shows the system specifications set for the prototype circuit. In this paper, an actual commercially available prototype circuit will be completed, and the specifications include the EMI specification EN55015. The efficiency of the current source is calculated from [4].

$$v_{ripple-pp} = \frac{I_{out}}{2 \cdot \pi \cdot f_{line} \cdot C_{O1}} \quad (4)$$

$$v_{ripple-pp-lowline} = \frac{0.45 \text{ A}}{2 \cdot \pi \cdot 60 \text{ Hz} \cdot (2 \cdot 470 \mu\text{F})} = 1.27 \text{ V} \quad (5)$$

$$v_{ripple-pp-highline} = \frac{0.45 \text{ A}}{2 \cdot \pi \cdot 50 \text{ Hz} \cdot (2 \cdot 470 \mu\text{F})} = 1.52 \text{ V} \quad (6)$$

From (4), it can be seen that the output voltage ripple is related to the average value of output current, line frequency and output capacitance of the flyback converter. According to the calculation, flyback converter operates at 230 Vac and 50 Hz for an LED string with output voltage 57 V and output rated current 450 mA, there will be a 1.52 V voltage ripple. Due to  $v_{B-min}$  equal to 0.6 V,  $v_{B-max}=2.12$  V, the power loss of block  $i_{source}$  at high line input voltage can be calculated as (7). Since the voltage and current at full load are 57 V and 0.45 A, respectively, the conversion efficiency of  $i_{source}$  at the high line input voltage is shown in (8). Due to the lower voltage ripple of 1.27 V as (5), the power loss of block  $i_{source}$  at low input voltage can be calculated as (9). The conversion efficiency of  $i_{source}$  at the low line input voltage is shown in (10).

$$P_{i-source} = i_{source} \cdot \frac{v_{B-min} + v_{B-max}}{2} = 0.61 \text{ W} \quad (7)$$

$$\eta_{i-source} = \frac{P_{LEDs}}{P_{i-source} + P_{LEDs}} = 97.67\% \quad (8)$$

$$P_{i-source} = i_{source} \cdot \frac{v_{B-min} + v_{B-max}}{2} = 0.45 \text{ W} \quad (9)$$

$$\eta_{i-source} = \frac{P_{LEDs}}{P_{i-source} + P_{LEDs}} = 98.38\% \quad (10)$$

The most difficult part of the flicker-free solution is to maintain high current regulation and wide dimming range at the same time. The design target of this prototype is to achieve a flicker rate of less than 3% at full load, and the conversion efficiency and power factor reach 89% and 0.9, respectively. Table 2 shows the specifications of the key components used in this paper. The larger the  $C_{O1}$ , the lower the output ripple and the higher the efficiency of the current source.

**Table 1** System specifications.

Item	Performance	Remarks
AC input range	90~264 Vac	
DC output voltage range	45~57 Vdc 450 mA	
Flicker Percentage	<3%	115 Vac/60 Hz & 230 Vac/50 Hz at LED 57 V /450 mA
Efficiency	89%	230Vac/50 Hz at LED 57V /450 mA
Power factor/THD	>0.9 <20%	115 Vac & 230 Vac 57 V output/450 mA
Dimming range	5%~100%	
Electromagnetic compatibility	EN55015	

**Table 2** Bill of material.

Symbol	Value
$Q_1$	SVF7N65CDTR;7 A/650 V
$Q_2$	AP10TN135N; 100 V/135 mA
$Q_3$	MMBT2907
$U_1$	LD7838
$U_2$	8051-based 8bit MCU
$C_{O1}$	2x470 $\mu\text{F}$ /63 V;
$R_S$	0.39 $\Omega$
$T_1$	POT3015; 1.1 mH; Turn ratio=48:18:7

### 3. RESULTS AND DISCUSSION

Fig. 8 shows the  $V_{LEDs}$  and  $i_{LEDs}$  of the proposed prototype circuit operating under different load voltages, different input voltages and load conditions. The higher the ripple amplitude, the lower the efficiency of the constant current source.

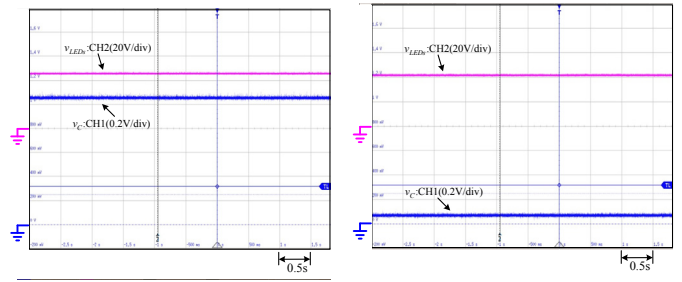
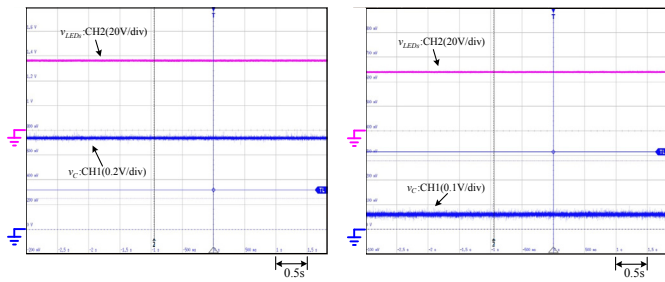
Fig. 9 shows the waveforms of  $v_A$ ,  $v_B$ , and  $v_E$  of the proposed prototype circuit operating at different input voltages, with a larger ripple at 230 Vac/50 Hz with a ripple amplitude of 1.4 V and a higher ripple of  $v_A$  at 115 Vac/60 Hz with a ripple amplitude of 1.2 V.

Fig. 10(a) shows the  $I_{LED}$  measurement waveform of the prototype circuit when switching between full brightness (full load) and full darkness (no load), while Fig. 10(b) shows the measurement waveform during progressive dimming.

Fig. 11 shows the measurement results of the dimming current error, which is higher due to the high input offset voltage of the internal  $OPA_2$  of MCU, but this does not cause strobing and is not easily detected by the human eyes. Fig. 12 shows the efficiency measurement results at different input voltages, output currents, and voltages. Based on the low loss of the constant current source, the overall conversion efficiency can be maximized for different load conditions.

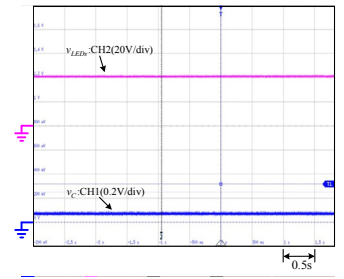
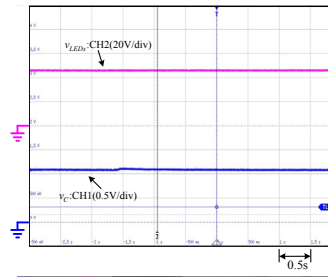
Figs. 13 and 14 are the measured results of the conductive and radiated EMI of this prototype circuit at different input voltages, which are in compliance with the EN55015 regulation required for mass production. Fig. 15 shows the comparison of Flicker Index, using LFA-3000 Light Flickering Analyzer from Everfine company, it can be found that the proposed structure has a very low Flicker Index compared to the traditional two-stage structure, and the Flicker Index can reach  $<0.1\%$  in the range of 20%~100% output current. The Flicker Index is under 0.1% at 20%~100% output current range.

Figs. 16 and 17 show the measurement results of power factor and current THD, both of which meet the design requirements.



(e) 100% dimming with 45 V LED and 115 Vac

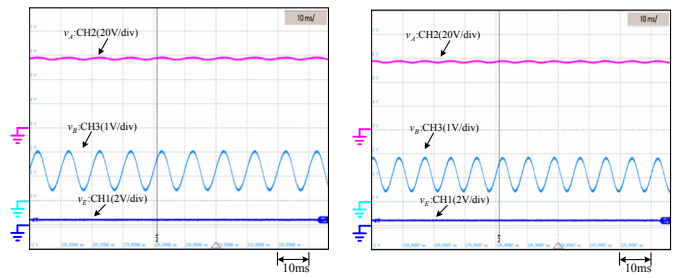
(f) 5% dimming with 45V LED and 115 Vac



(g) 100% dimming with 45 V LED and 230 Vac

(h) 5% dimming with 45 V LED and 230 Vac

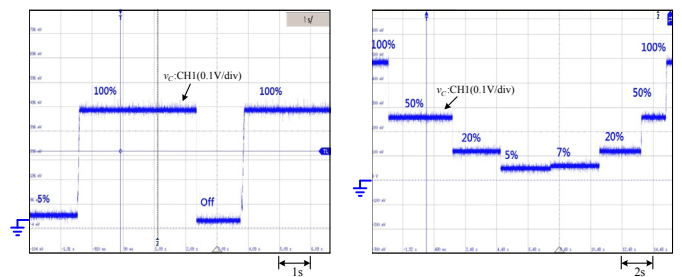
Fig. 8. Waveforms of LED voltage and  $v_C$  during dimming



(a) at input voltage 230 Vac

(b) at input voltage 115 Vac

Fig. 9 Waveforms of  $v_A$ ,  $v_B$ , and  $v_E$  at full load



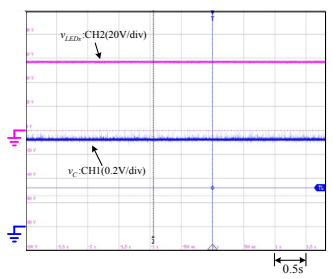
(a) when dimming On/Off

(b) continuous dimming

Fig. 10 Waveforms of  $v_C$  with dimming

(a) 100% dimming with 57 V LED and 115 Vac

(b) 5% dimming with 57 V LED and 115 Vac



(c) 100% dimming with 57 V LED and 230 Vac

(d) 5% dimming with 57 V LED and 230 Vac

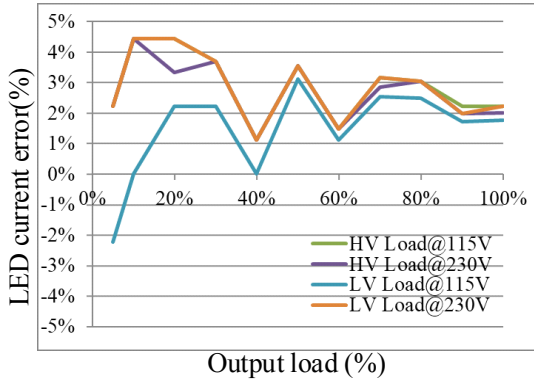


Fig. 11 Current error at different LED voltage and dimming conditions

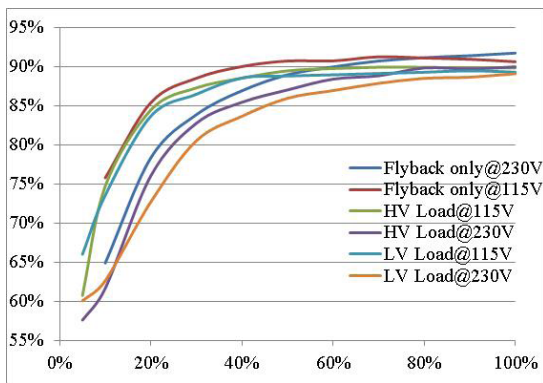
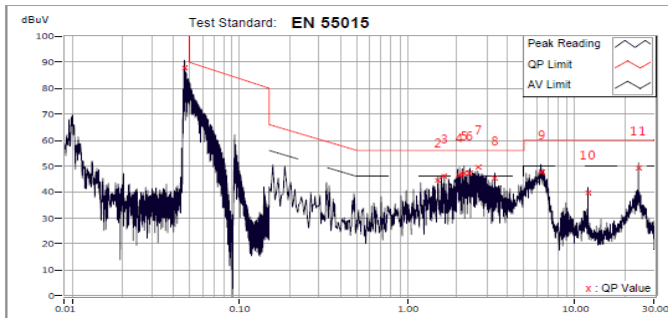
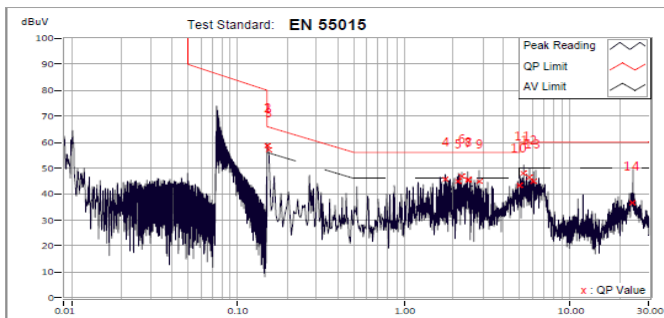


Fig. 12 Comparison of the conversion efficiency of the proposed method

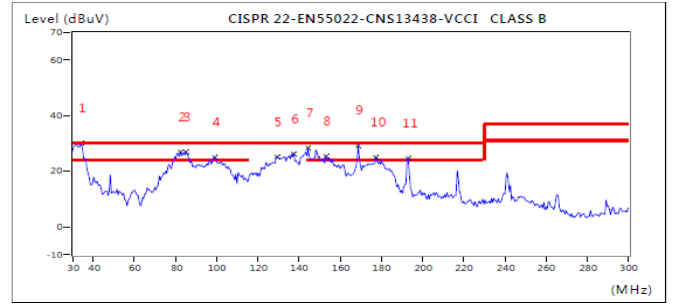


(a) at low line (115 Vac)

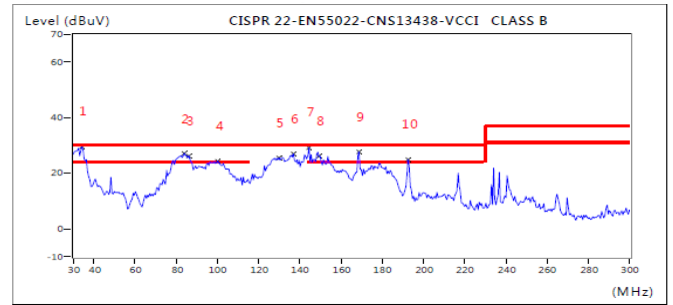


(b) at high line (230 Vac)

Fig. 13 Measurement results of conduction EMI



(a) at low line (115 Vac)



(b) at high line (230 Vac)

Fig. 14 Measurement results of radiation EMI emissions

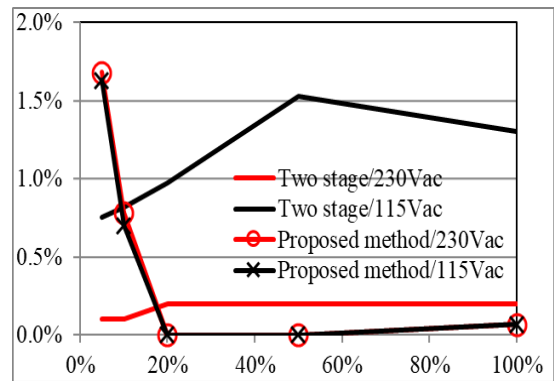


Fig. 15 Flicker percentage comparison

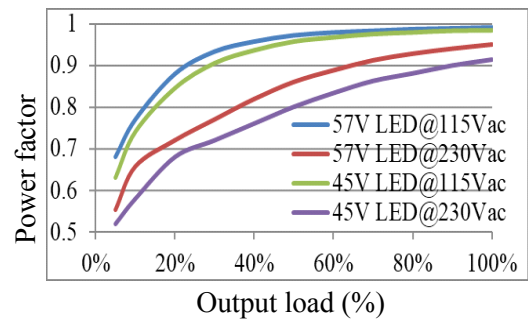


Fig. 16 Power factor at different input voltages, output voltages, and dimming currents

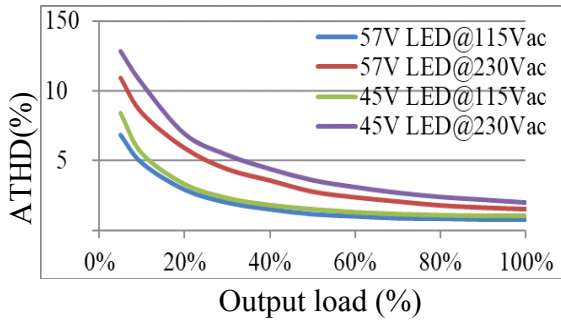


Fig. 17 ATHD for different input voltages, output voltages and dimming currents

#### 4. CONCLUSION

In this study, a novel high-efficiency LED driver is proposed, which includes a PFC flyback converter and a linear constant-current LED driver circuit. The results of the prototype circuit verified that the full-load conversion efficiency reached 90% and the overall power conversion efficiency improved by 7.5% compared to the conventional two-stage structure. According to the measurement results from the flicker tester, the maximum flicker percentage of the two-stage LED driver is 1.5% in the load range of 20% to 100%. The proposed new method has a percentage of flicker index under 0.1% in the load range of 20%~100%, which is significantly lower than the original two-stage structure. And the number of components in the proposed circuit is less than the traditional two-stage structure.

#### Abbreviations

Symbol and variable	Definition
$Q_1$	Main switch of flyback
$Q_2$	Constant current source transistor
$Q_3$	Feedback control transistor
$T_1$	Main transformer of flyback converter
$D_{O1}$	Rectifier diode of flyback converter
$V_{in}$	Input DC voltage from the bridge rectifier
$V_{LEDS}$	Total forward voltage of LED string
$i_{LEDS}$	The forward current of LED string
$v_{ds}$	Drain-source voltage of constant current source transistor $Q_3$
$v_{ds-min}, v_{ds-max}$	Minimum and maximum drain-source voltage of constant current source transistor $Q_3$ , respectively
$i_{source}$	constant current source
$v_A$	the output voltage of flyback converter
$v_B$	The voltage of current source
$v_C$	The voltage of current seasoning resistor
$v_D$	The output voltage of S/H circuit
$v_E$	The output of the feedback compensator

$v_F, v_G$	The flyback compensation voltage divider networks
$i_{ref}$	The reference of constant current source
$V_{ref}$	The reference voltage of constant current source
$v_{B-max}, v_{B-min}$	The maximum and minimum voltage of current source, respectively
$v_{ripple-pp}$	Peak to peak voltage of $v_A$
$v_{ripple-pp-lowline}, v_{ripple-pp-highline}$	Peak to peak voltage of $v_A$ at high line input voltage and low line input voltage, respectively
$P_{LEDS}$	Power of LED load
$P_{i-source}$	Power loss of constant current source
$\eta_{i-source}$	Conversion efficiency of constant current source
$R_S$	Current seasoning resistor of constant current source
$R_{up}, R_{dn1}, R_{dn2}$	The resistors of the feedback network
$OPA_1, OPA_2$	Variation rang of $f_{sw}$

#### REFERENCES

- Cheng, C. A., Cheng, H. L., & Chung, T. Y. (2014). "A novel single-stage high-power-factor LED street-lighting driver with coupled inductors." *IEEE Transactions on Industry Applications*, **50**(5), 3037-3045.
- Dong, H., Xie, X., Peng, K., Li, J., & Zhao, C. (2014, October). "Feed-forward dynamic compensation control for single-stage PFC LED driver to eliminate flicker to human eyes during AC input voltage variation." In *IECON 2014-40th Annual Conference of the IEEE Industrial Electronics Society*. IEEE, 1460-1465.
- Fang, P., & Liu, Y. F. (2014, March). "An electrolytic capacitor-free single stage Buck-Boost LED driver and its integrated solution." In *2014 IEEE Applied Power Electronics Conference and Exposition-APEC 2014*. IEEE, 1394-1401.
- Fang, P., & Liu, Y. F. (2016). "Energy channeling LED driver technology to achieve flicker-free operation with true single stage power factor correction." *IEEE Transactions on Power Electronics*, **32**(5), 3892-3907.
- Fang, P., Qiu, Y. J., Wang, H., & Liu, Y. F. (2016). "A single-stage primary-side-controlled off-line flyback LED driver with ripple cancellation." *IEEE Transactions on Power Electronics*, **32**(6), 4700-4715.
- Fang, P., Sheng, B., Webb, S., Zhang, Y., & Liu, Y. F. (2018). "LED driver achieves electrolytic capacitor-less and flicker-free operation with an energy buffer unit." *IEEE transactions on power electronics*, **34**(7), 6777-6793.
- Fang, P., White, B., Fiorentino, C., & Liu, Y. F. (2013, September). "Zero ripple single stage AC-DC LED driver with unity power factor." In *2013 IEEE Energy Conversion Congress and Exposition*. IEEE, 3452-3458.
- Fu, J., Wang, G., Wang, S., Chen, Z., & Shi, L. (2018, June). "A Novel AC Direct Linear LED Driver with Unity Power Factor, Low In-

- put Current THD, Low Light Flicker and Low Profile.” In *PCIM Europe 2018; International Exhibition and Conference for Power Electronics, Intelligent Motion, Renewable Energy and Energy Management*. VDE, 1-7.
- Gao, Y., Li, L., & Mok, P. K. (2015, June). “A 5.5 W AC input converter-free LED driver with 82% low-frequency-flicker reduction, 88.2% efficiency and 0.92 power factor.” In *2015 Symposium on VLSI Circuits (VLSI Circuits)*. IEEE, C286-C287.
- He, J., Ruan, X., & Zhang, L. (2016). “Adaptive voltage control for bidirectional converter in flicker-free electrolytic capacitor-less AC–DC LED driver.” *IEEE Transactions on Industrial Electronics*, **64**(1), 320-324.
- Hu, Q., & Zane, R. (2010, February). “A 0.9 PF LED driver with small LED current ripple based on series-input digitally-controlled converter modules.” In *2010 Twenty-Fifth Annual IEEE Applied Power Electronics Conference and Exposition (APEC)*. IEEE, 2314-2320.
- Hu, Q., & Zane, R. (2011, September). “Off-line LED driver with bidirectional second stage for reducing energy storage.” In *2011 IEEE Energy Conversion Congress and Exposition*. IEEE, 2302-2309.
- Li, Y., Han, J., & Sanders, S. (2018, September). “A low cost AC direct LED driver with reduced flicker using triac.” In *2018 IEEE Energy Conversion Congress and Exposition (ECCE)*. IEEE, 4738-4743.
- Liu, P. J., Hsu, S. R., Chang, C. W., Liao, C. Y., & Chien, L. H. (2015, November). “Dimmable white LED driver with adaptive voltage feedback control.” In *2015 IEEE 2nd International Future Energy Electronics Conference (IFEEC)*. IEEE, 1-4.
- Ruan, X., Wang, B., Yao, K., & Wang, S. (2010). “Optimum injected current harmonics to minimize peak-to-average ratio of LED current for electrolytic capacitor-less AC–DC drivers.” *IEEE Transactions on Power Electronics*, **26**(7), 1820-1825.
- Wang, S., Ruan, X., Yao, K., Tan, S. C., Yang, Y., & Ye, Z. (2011). “A flicker-free electrolytic capacitor-less AC–DC LED driver.” *IEEE Transactions on Power Electronics*, **27**(11), 4540-4548.
- Wang, L., Zhang, B., & Qiu, D. (2017, March). “A novel flicker-free AC-DC LED driver without electrolytic capacitor.” In *2017 IEEE International Conference on Industrial Technology (ICIT)*. IEEE, 370-375.
- Wilkins, A., Veitch, J., & Lehman, B. (2010, September). “LED lighting flicker and potential health concerns: IEEE standard PAR1789 update.” In *2010 IEEE Energy Conversion Congress and Exposition*, IEEE, 171-178.
- Yan, T., Xu, J., Liu, X., Zhou, G., & Gao, J. (2014). “Flicker-free transformerless LED driving circuit based on quadratic buck PFC converter.” *Electronics Letters*, **50**(25), 1972-1974.
- Yang, Y., Ruan, X., Zhang, L., He, J., & Ye, Z. (2013). “Feed-forward scheme for an electrolytic capacitor-less AC/DC LED driver to reduce output current ripple.” *IEEE Transactions on Power Electronics*, **29**(10), 5508-5517.
- [1] Application Note, “Understanding Power MOSFET Parameters,” Taiwan Semiconductor, [Online]. Available: [www.taiwansemi.com](http://www.taiwansemi.com)
- [2] Application Note, “Versatile High Precision Programmable Current Sources Using DACs, Op Amps, and MOSFET Transistor,” Analog Devices Inc., [Online]. Available: [www.analog.com/](http://www.analog.com/)
- [3] Datasheet, “AP10TN135N,” Advanced Power Electronics, [Online]. Available: [www.a-power.com.tw](http://www.a-power.com.tw)
- [4] Application Note, “55 W flyback converter design using the IRS2982S controller,” Infineon, [Online]. Available: [www.infineon.com/](http://www.infineon.com/)